J Gastric Cancer. 2022 Oct;22(4):348-368
https://doi.org/10.5230/jgc.2022.22.e31
pISSN 2093-582X·eISSN 2093-5641

jgc Journal of Gastric Cancer

Original Article

PLK2 Single Nucleotide Variant in Gastric Cancer Patients Affects miR-23b-5p Binding

Pia Pužar Dominkuš [1], **Aner Mesic** [2], **Petra Hudler** [1]

[1]University of Ljubljana, Faculty of Medicine, Institute of Biochemistry and Molecular Genetics, Ljubljana, Slovenia
[2]University of Sarajevo, Faculty of Science, Department of Biology, Sarajevo, Bosnia and Herzegovina.

Received: Mar 8, 2022
Revised: Jul 28, 2022
Accepted: Aug 10, 2022
Published online: Sep 26, 2022

Correspondence to
Petra Hudler
University of Ljubljana, Faculty of Medicine, Institute of Biochemistry and Molecular Genetics, Vrazov trg 2, 1000 Ljubljana, Slovenia.
Email: petra.hudler@mf.uni-lj.si

ORCID iDs
Pia Pužar Dominkuš
https://orcid.org/0000-0002-4552-7565
Aner Mesic
https://orcid.org/0000-0002-2263-0420
Petra Hudler
https://orcid.org/0000-0002-2546-0674

Funding
This study was supported by the Slovenian research agency (ARRS) Research Programme Grant (P1-390) and a Young Researcher Grant to Pia Pužar Dominkuš.

Conflict of interest
No potential conflict of interest relevant to this article was reported.

ABSTRACT

Purpose: Chromosomal instability is a hallmark of gastric cancer (GC). It can be driven by single nucleotide variants (SNVs) in cell cycle genes. We investigated the associations between SNVs in candidate genes, *PLK2*, *PLK3*, and *ATM,* and GC risk and clinicopathological features.
Materials and Methods: The genotyping study included 542 patients with GC and healthy controls. Generalized linear models were used for the risk and clinicopathological association analyses. Survival analysis was performed using the Kaplan-Meier method. The binding of candidate miRs was analyzed using a luciferase reporter assay.
Results: The *PLK2* $\mathbf{C}_{rs15009}$-$\mathbf{C}_{rs963615}$ haplotype was under-represented in the GC group compared to that in the control group (P_{corr}=0.050). Male patients with *the PLK2* rs963615 CT genotype had a lower risk of GC, whereas female patients had a higher risk (P=0.023; P=0.026). The *PLK2* rs963615 CT genotype was associated with the absence of vascular invasion (P=0.012). The *PLK3* rs12404160 AA genotype was associated with a higher risk of GC in the male population (P=0.015). The *ATM* $\mathbf{T}_{rs228589}$-$\mathbf{A}_{rs189037}$-$\mathbf{G}_{rs4585}$ haplotype was associated with a higher risk of GC (P<0.001). The *ATM* rs228589, rs189037, and rs4585 genotypes TA+AA, AG+GG, and TG+GG were associated with the absence of perineural invasion (P=0.034). *In vitro* analysis showed that the cancer-associated miR-23b-5p mimic specifically bound to *the PLK2* rs15009 G allele (P=0.0097). Moreover, low miR-23b expression predicted longer 10-year survival (P=0.0066) in patients with GC.
Conclusions: *PLK2*, *PLK3*, and *ATM* SNVs could potentially be helpful for the prediction of GC risk and clinicopathological features. *PLK2* rs15009 affects the binding of miR-23b-5p. MiR-23b-5p expression status could serve as a prognostic marker for survival in patients with GC.

Keywords: Gastric cancer; Genetic variation; Chromosomal instability; Cell cycle genes; MiR-23b-5p

INTRODUCTION

Gastric cancer (GC) is the fourth most common cause of cancer-related death worldwide [1]. GC is a complex, multifactorial disease influenced by intricate interactions between environmental and genetic factors [2]. In a large study conducted by The Cancer Genome Atlas (TCGA) involving 295 patients with gastric adenocarcinoma, approximately 50% of

jgc Journal of Gastric Cancer

Author Contributions

Conceptualization: H.P., D.P.P.; Funding acquisition: H.P.; Methodology: D.P.P., M.A.; Project administration: H.P.; Supervision: H.P.; Visualization: H.P., D.P.P.; Writing - original draft: H.P., D.P.P., M.A.; Writing - review & editing: H.P., D.P.P., M.A.

tumors were characterized by chromosomal instability [3]. It is believed that this form of genomic instability leads to long-term accumulation of genomic changes, which eventually results in the transformation of normal cells into malignant cells [4]. Recent studies have suggested that chromosomal instability can be driven by low-penetrating changes, such as single nucleotide variants (SNVs) in cell cycle and DNA repair genes [5,6], as these are extremely polymorphic [7].

Cyclins and cyclin-dependent kinases, Aurora kinases, checkpoint kinases, and other kinases, such as polo-like kinases (PLK) and ataxia telangiectasia mutated protein (ATM), are essential for cell cycle progression and response to stress. PLK2 is involved in centriole duplication and the G1/S phase transition, whereas PLK3 is required for entry into the S phase and cytokinesis [8,9]. Both kinases appear to act as tumor suppressors. *PLK2* is transcriptionally silenced through promoter methylation in hematologic B-cell malignancies [10], acute myeloid leukemia [11], and hepatocellular carcinoma [12]. *PLK3* has been shown to be downregulated in B cells during *Helicobacter pylori* infection, a well-known GC risk factor [13]. *PLK3* mRNA is undetectable or significantly downregulated compared to paired normal tissue in lung carcinomas [14], head and neck carcinoma [15], and carcinogen-induced rat colon tumors [16]. ATM is involved in cellular response to DNA damage, cell cycle regulation, chromatin remodelling, and apoptosis [17,18]. Germline mutations in *ATM* result in ataxia telangiectasia syndrome, which manifests as a lifetime increased cancer risk [19]. A genome-wide association study performed on a European population demonstrated the association between loss-of-function SNVs in *ATM* and GC and showed that cancer occurs at a significantly earlier age in those carrying these variants than in non-carriers [20].

Low penetrating SNVs in these genes in combination with environmental factors could be crucial biomarkers to aid in disease prevention and early intervention strategies. Our aim was to assess the association of candidate SNVs in cell cycle genes, *PLK2*, *PLK3*, and *ATM,* with GC risk and clinicopathological features of the patients in a case-control study. Relevant associations were further evaluated using *in silico* analysis and *in vitro* luciferase reporter assay.

MATERIALS AND METHODS

Study populations

A total of 221 patients with gastric adenocarcinoma and 321 healthy individuals were enrolled in this retrospective, case-control study. The diagnosis was confirmed by histological examination of the tissues removed during surgery. The patients underwent surgery at the Department of Abdominal Surgery and the Department of Thoracic Surgery at the University Medical Center Ljubljana, Jesenice Hospital, Hospital Dr. Petra Držaja, and the Ljubljana Institute of Oncology. The controls were matched by ethnicity, free from any personal history of GC or other malignant neoplasms, and unrelated to the patients and to each other. Tissue and blood samples were frozen at −80°C until use.

Human rights statement and informed consent

All procedures followed were in accordance with the ethical standards of the responsible committee on human experimentation (institutional and national) and the Helsinki Declaration of 1964 and later versions. This study was approved by the Republic of Slovenia National Medical Ethics Committee (No. 0120-59/2019/3). This was a retrospective study.

https://doi.org/10.5230/jgc.2022.22.e31

jgc Journal of Gastric Cancer

DNA isolation

Genomic DNA was isolated from adjacent non-tumor gastric and tumor tissue samples from patients with GC and peripheral blood samples of controls using the Wizard Genomic DNA Purification Kit (Promega Corporation, Madison, WI, USA) following the manufacturer's instructions. The concentration and purity of isolated DNA were determined spectrophotometrically using a Synergy H4 Hybrid Microplate Reader (BioTek Instruments, Inc., Winooski, VT, USA).

SNV selection and genotyping

Seven SNVs in cell cycle genes were selected for genotyping: rs963615 and rs15009 in *PLK2*; rs17883304 and rs1204160 in *PLK3*; and rs228589, rs189037, and rs4585 in *ATM*. The SNVs were selected according to the following criteria: a) previous reports of gene associations with GC, b) minor allele frequency (MAF) of ≥10% in Utah residents with Northern and Western European ancestry (CEU) population according to the 1000 Genomes Project Phase 3 project, and c) *in silico* analysis of functional annotations in the selected candidate regions using the publicly available single nucleotide polymorphism selection tool, SNPinfo (http://www.niehs.nih.gov/snpinfo) [21]. The SNVs were genotyped using the following TaqMan allelic discrimination assays, which were supplied as predesigned SNV genotyping assays: C_8962866_10 (rs963615), C_2839927_1_ (rs15009), C_63720915_10 (rs17883304), C_159308_10 (rs12404160), C_2283144_1_ (rs228589), C_2283145_10 (rs189037), C_1039793_20 (rs4585) (Applied Biosystems, Foster City, CA, USA). Genotyping was performed in 5-μL reaction mixtures containing 20x SNV genotyping assay, 2x Taq-Man Genotyping Master Mix (Applied Biosystems), and 10 ng of genomic DNA. The polymerase chain reaction (PCR) was performed according to the manufacturer's protocol using ViiA™ 7 Real-Time PCR System and QuantStudio™ Real-Time PCR Software (Applied Biosystems) with the following cycling conditions: 60°C for 30 seconds, 95°C for 10 minutes followed by 45 cycles at 95°C for 15 seconds, 60°C for 1 minute, and 60°C for 30 seconds. Random samples were selected and re-genotyped to confirm the consistency of obtained genotypes.

Haplotype analysis

For SNVs in *ATM*, *PLK2*, and *PLK3*, raw genotyping data for genetic variants, rs228589, rs189037, and rs4585 in *ATM*; rs15009 and rs963615 in *PLK2*; and rs17883304 and rs12404160 in *PLK3,* were extracted. to perform haplotype analysis and generate the haplotype block structure, which entailed corrections for multiple comparisons by 10000 permutations, Haploview software version 4.2. [22] and SNP tools V1.80 (MS Windows, Microsoft Excel) [23] were used. In this regard, the solid spine of the linkage disequilibrium (LD) algorithm with a minimum Lewontin D′ value of 0.8 was chosen. To correct the occurrence of type I errors (false positive results), a permutation procedure was performed using Haploview (10000 permutations). This approach enables correction for multiple testing, but also considers the correlation between markers. Hence, permutation correction is less conservative than Bonferroni correction; however, it is suitable for independent tests with multiple markers [24].

In silico SNV analysis

The functional effects of intron and UTR SNVs were evaluated using the following publicly available bioinformatics tools: a) PROMO software within the ALGGEN (Algorithmics and Genetics Group) web server [25,26] for the search for putative transcription factor motifs. We built the search using the following parameters: human species, all motifs, and all factors; b) MirSNP database for the prediction of miR-binding sites affected by SNVs [27].

https://doi.org/10.5230/jgc.2022.22.e31

jgc Journal of Gastric Cancer

The miRANDA algorithm used in the MirSNP database uses criteria where the seed region contains at least seven nt long. However, we additionally excluded miRs that could potentially bind to one allele with a 6 nt seed region, as this possibility has been observed and described previously in the literature [28]. For *PLK2,* which lies on the reverse strand, all alleles are reported in the forward orientation. Gene orientation was considered for *in silico* functional analysis. Sequences for *in silico* analysis of the studied SNVs in FASTA format were extracted from Ensembl Release 99 (http://www.ensembl.org) [29].

Dual Luciferase reporter assay

The *PLK2* 3' UTR region with the wild-type (Wt) or polymorphic allele (Var) was cloned into the dual luciferase reporter vector pmirGLO (Promega Corporation). GC cells, MKN45, obtained from the Japanese Collection of Research Bio Resources Cell Bank (JCRB, Osaka, Japan) were transfected with miR-23a-5p, miR-23b-5p, or negative control mimics (Dharmacon, Lafayette, CO, USA) and pmirGLO-PLK2-3'UTR Wt, pmirGLO-PLK2-3'UTR Var, or pmirGLO as negative controls, using GenMute siRNA Transfection Reagent (SignaGen Laboratories, MD, USA) according to the manufacturer's protocol. Luciferase activity was measured using the Dual Luciferase Reporter Assay (Promega Corporation) on the Synergy H4 Hybrid Microplate Reader (BioTek) luminometer, 48 hours after transfection. Experiments were performed in triplicate and replicated four times. Data are represented as the mean ± standard deviation and were compared using GraphPad Prism version 8.0.2 for Windows. Statistical significance was set at $P<0.05$.

Statistical analysis

The agreement of genotype frequencies with Hardy-Weinberg equilibrium (HWE) and the differences in genotype distribution between cases and controls were calculated using the chi-squared test. Minor genotype and allele frequencies for candidate SNVs were compared to the frequencies in populations from the 1000 Genome Project Phase 3 release. A generalized linear model was used to calculate odds ratios (ORs) and 95% confidence intervals (CIs) to examine the association of selected SNVs with the risk of GC and clinicopathological features. Dominant, recessive, and co-dominant genetic models were used for the analysis, depending on the genotype frequencies. All associations were calculated using R studio version 3.5.3 [30] and the SNPAssoc package for R [31]. When more associations were significant for one SNV, the genetic model with the lowest Akaike information criterion value was selected [32]. The associations between SNVs genotypes and overall patient survival were estimated using the Kaplan–Meier (KM) method and log-rank test using GraphPad Prism version 8.0.2 for Windows (GraphPad Software, San Diego, CA, USA, www.graphpad.com). *S*tatistical significance was set at $P<0.05$. KM miR survival curves were generated using the KM Plotter online tool (https://kmplot.com) [33] and TCGA datasets (n=436 patients with GC). The TCGA dataset is available using the following link: https://portal.gdc.cancer.gov/. Differential expression of hsa-miR-23b-5p in tumors vs. normal or high vs. low-grade GC samples was extracted from the dbDEMC 3.0 database (https://www.biosino.org/dbDEMC/index) [34]. Expression datasets in dbDEMC are based on microarray or miRNA-seq platforms obtained from public repositories, including Gene Expression Omnibus (GEO), Sequence Read Archive, ArrayExpress, and TCGA.

https://doi.org/10.5230/jgc.2022.22.e31

jgc Journal of Gastric Cancer

RESULTS

Characteristics of study participants and genotype distributions of studied SNVs

A total of 221 patients with GC were enrolled in this study. Clinical and histological data were extracted from registered medical records and are presented in **Table 1**. Male patients accounted for 62.25%, and female patients accounted for 37.75% of the study cohort. Their mean age at diagnosis was 67.3 years. Data on histological type, according to Lauren's classification; location; grade of differentiation; and vascular, perineural, and lymphatic invasion were included in the study. SNVs from the three cell cycle genes, *PLK2*, *PLK3*, and *ATM,* are presented in **Table 2**. All selected SNVs were located in the non-coding regions of the genes. Genotype and allele frequencies in patients with GC and controls were comparable to those in populations from public databases (**Supplementary Fig. 1**). The distribution of genotype frequencies and HWE in patients with GC and controls for each studied SNV were analyzed using the chi-square test (**Supplementary Table 1**). Genotype frequencies did not deviate from the HWE (P>0.05).

Table 1. Clinicopathological features of patients

Parameters	Values
Age (yr) (n=203)	67.30±12.50
Sex (n=204)	
Male age	127 (62.25)/67.36±12.50
Female age	77 (37.75)/67.34±12.52
Lauren's classification (n=179)	
Intestinal	88 (49.16)
Mixed and diffuse	91 (50.84)
Location (n=158)	
Oesophageal junction	29 (18.35)
Stomach	129 (81.65)
Grade of differentiation (n=164)	
Low grade	111 (67.68)
High grade	53 (32.32)
Vascular invasion (n=126)	
Present	81 (64.29)
Absent	45 (35.71)
Perineural invasion (n=93)	
Present	47 (50.54)
Absent	46 (49.46)
Lymphatic invasion (n=94)	
Present	86 (91.49)
Absent	8 (8.51)

Values are presented as number of patients (%) or mean ± standard deviation.

Table 2. Allele information and chromosomal positions for studied SNVs

Gene	SNV	Alleles*	SNV location	Chromosomal position†
PLK2	rs963615	CT	5′ UTR	Chr.5:58460109
	rs15009	CG	3′ UTR	Chr.5:58454523
PLK3	rs17883304	AC	Intron	Chr.1:44802360
	rs12404160	GA	Intron	Chr.1:44802710
ATM	rs228589	TA	Intron	Chr.11:108222481
	rs189037	AG	5′ UTR	Chr.11:108223106
	rs4585	TG	3′ UTR	Chr.11:108368901

SNV = single nucleotide variation.
*The ancestral allele of the EUR population is written first. Alleles have been reported in the forward orientation.
†According to the GRCh38.p13 reference genome build.

https://doi.org/10.5230/jgc.2022.22.e31

jgc Journal of Gastric Cancer

PLK2 and *PLK3* SNVs are associated with GC risk in male and female populations

We performed analyses based on generalized linear models to evaluate the association between candidate SNV genotypes and GC risk. Genotyping was performed on DNA isolated from non-tumor gastric tissues (**Table 3**). There were no significant associations between the cell cycle genes SNVs, *PLK2* rs963615, rs15009, *PLK3* rs17883304, and rs12404160, or *ATM* rs228589, rs189037, and rs4585 and GC risk. In the stratified analysis, there were significant associations between the *PLK2* rs963615 CT genotype and lower GC risk in the male population according to the overdominant genetic model [(CC+TT):CT] (OR=0.59, 95% CI=0.37–0.93, P=0.023) and higher GC risk in the female population in the same genetic model [(CC+TT):CT] (OR = 2.03, 95% CI=1.09–3.80, P=0.026). A significant association was also found between the *PLK3* rs12404160 AA genotype and a higher GC risk in the male population, according to the recessive genetic model [(GG+GA):AA] (OR=3.55, 95% CI=1.26–10.04, P=0.015).

ATM, *PLK2*, and *PLK3* haplotypes are associated with GC risk

For haplotype analysis, a single haplotype block was created that included either *PLK2*, *PLK3,* or *ATM* SNVs with an average Lewontin D' > 0.8 (D'=1.0 value shows the strongest LD between the two polymorphisms) (**Fig. 1**). Haplotype frequencies of the cases and controls are presented in **Table 4**. The frequency of *the PLK2* $\mathbf{C}_{rs15009}$-$\mathbf{C}_{rs963615}$ haplotype was lower in the GC group than that in the control group, with borderline significance (P_{corr}=0.050). This association was marginal; therefore, our results should be interpreted with caution and further validated in a larger cohort. The frequency of the *PLK3* $\mathbf{A}_{rs17883304}$-$\mathbf{T}_{rs12404160}$ haplotype was significantly lower in the GC group than that in the control group (P_{corr}=0.001). Additionally, the frequency of the *ATM* $\mathbf{A}_{rs228589}$-$\mathbf{G}_{rs189037}$-$\mathbf{T}_{rs4585}$ haplotype was significantly lower, and that of the $\mathbf{T}_{rs228589}$-$\mathbf{A}_{rs189037}$-$\mathbf{G}_{rs4585}$ haplotype was significantly higher in the GC group than in the control group (P_{corr}<0.001).

PLK2 and *ATM* SNVs are associated with the presence of vascular and perineural invasion

Association analysis between SNVs genotypes and clinicopathological tumor features was performed on genotyping results from gastric tumor tissue DNA, given that variations in tumor tissue define the behavior and characteristics of the tumor. The categories with the most significant results are presented in **Table 5**. The non-significant results are shown in **Supplementary Table 2**. Genotype CT in *PLK2* rs963615 was significantly associated with the absence of vascular invasion according to the overdominant genetic model [(CC + TT):CT)] (OR=0.38, 95% CI=0.18–0.81, P=0.012). Genotypes TA+AA, AG+GG, and TG+GG in *ATM* rs228589, rs189037, and rs4585, respectively, were significantly associated with the absence of perineural invasion (OR=0.39, 95% CI=0.16–0.95, P=0.034) according to the dominant genetic models [TT:(TA+AA)], [AA:(AG+GG)], and [TT:(TG+GG)], respectively.

Associations between candidate SNV genotypes and survival prognosis of patients

The survival interval in our GC patient cohort ranged from 1.6–133.5 months (mean, 40.0 months). Survival analysis was performed to examine the effect of candidate SNVs on the prognosis of patients with GC (**Fig. 2**). Analysis was performed on SNVs where each genotype group comprised a minimum of five participants. No significant associations were found between candidate SNV genotypes and overall survival in patients with GC. However, a trend was observed for patients with the *PLK2* rs15009 GG genotype, who had a 10-year survival

https://doi.org/10.5230/jgc.2022.22.e31

jgc Journal of Gastric Cancer

Table 3. Association between *PLK2*, *PLK3* and *ATM* candidate SNV genotypes and gastric cancer risk for all patients with GC and stratified male and female patients with GC

Genotypes	All patients with GC		Male patients with GC		Female patients with GC	
	OR (95% CI)	P-value	OR (95% CI)	P-value	OR (95% CI)	P-value
rs963615 (*PLK2*)						
CC	1 (ref)	0.696	1 (ref)	0.076	1 (ref)	0.073
CT	0.92 (0.64–1.32)		0.59 (0.37–0.95)		1.95 (1.03–3.72)	
TT	0.75 (0.37–1.53)		0.99 (0.43–1.25)		0.73 (0.21–2.55)	
CC:(CT+TT)*	0.89 (0.63–1.26)	0.517	0.64 (0.41–1.01)	0.052	1.68 (0.91–3.10)	0.099
(CC+CT):TT†	0.78 (0.39–1.56)	0.475	1.24 (0.56–2.76)	0.601	0.54 (0.16–1.83)	0.308
(CC+TT):CT‡	0.95 (0.67–1.36)	0.775	**0.59 (0.37–0.93)**	**0.023**	2.03 (1.09–3.80)	**0.026**
rs15009 (*PLK2*)						
CC	1 (ref)	0.254	1 (ref)	0.495	1 (ref)	0.313
CG	0.74 (0.51–1.07)		0.76 (0.47–1.21)		0.63 (0.33–1.19)	
GG	0.93 (0.52–1.65)		0.81 (0.39–1.68)		1.03 (0.35–3.04)	
CC:(CG+GG)*	0.77 (0.54–1.09)	0.145	0.77 (0.49–1.19)	0.241	0.68 (0.37–1.26)	0.219
(CC+CG):GG†	1.09 (0.63–1.88)	0.751	0.94 (0.47–1.87)	0.854	1.32 (0.47–3.70)	0.600
(CC+GG):CG‡	0.75 (0.53–1.06)	0.102	0.79 (0.51–1.23)	0.300	0.62 (0.34–1.15)	0.128
rs17883304 (*PLK3*)						
AA	1 (ref)	0.670	1 (ref)	0.503	1 (ref)	0.907
AC	0.85 (0.58–1.24)		0.88 (0.55–1.43)		1.04 (0.55–2.06)	
CC	1.11 (0.40–3.05)		1.72 (0.58–5.08)		0.49 (0.05–7.06)	
AA:(AC+CC)*	0.87 (0.60–1.26)	0.460	0.96 (0.61–1.51)	0.853	1.00 (0.54–1.98)	0.928
(AA+AC):CC†	1.17 (0.43–3.19)	0.762	1.79 (0.61–5.23)	0.290	0.48 (0.05–6.88)	0.684
(AA+CC):AC‡	0.84 (0.58–1.24)	0.383	0.85 (0.53–1.38)	0.516	1.06 (0.55–2.08)	0.835
rs12404160 (*PLK3*)						
GG	1 (ref)	0.171	1 (ref)	0.050	1 (ref)	0.830
GA	1.00 (0.68–1.48)		1.03 (0.63–1.70)		1.19 (0.61–2.33)	
AA	2.42 (0.95–6.19)		3.59 (1.25–10.30)		1.50 (0.20–11.07)	
GG:(GA+AA)*	1.10 (0.76–1.60)	0.617	1.23 (0.77–1.96)	0.394	1.21 (0.63–2.33)	0.570
(GG+GA):AA†	2.42 (0.96–6.13)	0.060	**3.55 (1.26–10.04)**	**0.015**	1.42 (0.19–10.31)	0.732
(GG+AA):GA‡	0.95 (0.64–1.40)	0.789	0.93 (0.57–1.52)	0.782	1.17 (0.60–2.28)	0.642
rs228589 (*ATM*)						
TT	1 (ref)	0.760	1 (ref)	0.568	1 (ref)	0.196
TA	0.88 (0.60–1.28)		1.05 (0.65–1.70)		0.69 (0.35–1.36)	
AA	1.01 (0.59–1.71)		0.73 (0.36–1.49)		1.56 (0.63–3.86)	
TT:(TA+AA)*	0.91 (0.64–1.30)	0.598	0.97 (0.61–1.54)	0.911	0.87 (0.47–1.61)	0.659
(TT+TA):AA†	1.08 (0.67–1.76)	0.750	0.71 (0.37–1.36)	0.297	1.86 (0.80–4.34)	0.147
(TT+AA):TA‡	0.88 (0.62–1.24)	0.460	1.15 (0.74–1.78)	0.537	0.62 (0.33–1.15)	0.129
rs189037 (*ATM*)						
AA	1 (ref)	0.965	1 (ref)	0.663	1 (ref)	0.357
AG	0.95 (0.65–1.39)		1.04 (0.64–1.68)		0.86 (0.44–1.68)	
GG	0.98 (0.58–1.65)		0.78 (0.39–1.53)		1.68 (0.67–4.21)	
AA:(AG+GG)*	0.96 (0.67–1.37)	0.806	0.97 (0.61–1.53)	0.895	1.03 (0.56–1.91)	0.928
(AA+AG):GG†	1.00 (0.62–1.63)	0.989	0.76 (0.41–1.41)	0.375	1.81 (0.77–4.27)	0.172
(AA+GG):AG‡	0.96 (0.67–1.36)	0.803	1.12 (0.72–1.74)	0.606	0.75 (0.40–1.40)	0.368
rs4585 (*ATM*)						
TT	1 (ref)	0.887	1 (ref)	0.913	1 (ref)	0.449
TG	1.04 (0.71–1.52)		1.10 (0.67–1.80)		0.95 (0.49–1.84)	
GG	1.14 (0.67–1.94)		1.00 (0.51–1.97)		1.72 (0.67–4.43)	
TT:(TG+GG)*	1.06 (0.74–1.53)	0.736	1.08 (0.68–1.72)	0.753	1.10 (0.59–2.03)	0.765
(TT+TG):GG†	1.12 (0.69–1.81)	0.656	0.95 (0.52–1.74)	0.862	1.76 (0.73–4.28)	0.209
(TT+GG)TG‡	1.00 (0.71–1.42)	0.994	1.10 (0.71–1.71)	0.670	0.84 (0.45–1.54)	0.565

ORs, 95% CIs; P-values, estimated using generalized linear models. Statistically significant values are highlighted in bold (P<0.05).
SNV = single nucleotide variation; GC = gastric cancer; OR = odds ratio; CI = confidence interval; Ref = reference homozygote.
*Dominant genetic model (common homozygote vs. rare homozygote + heterozygote); †Recessive genetic model (rare homozygote vs. common homozygote + heterozygote); ‡Overdominant genetic model (heterozygote vs. common homozygote + rare homozygote).

rate of 63.5% in comparison to the patients with the CG or CC genotype (survival rate, 15.7% and 20%, respectively) (P=0.337, **Fig. 2B**).

https://doi.org/10.5230/jgc.2022.22.e31

jgc Journal of Gastric Cancer

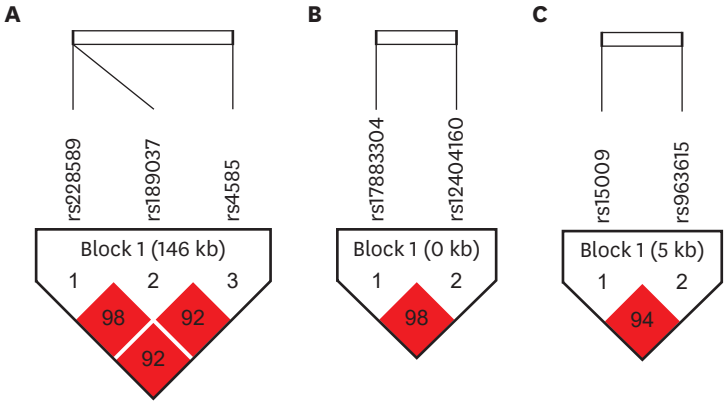

Fig. 1. LD structure between variants in the (A) *ATM*, (B) *PLK2* and (C) *PLK3* genes. The color image represents Lewontin D' values and LOD. Red squares indicate LOD≥2 and D'=1. Strong LD between a pair of SNVs is represented using red color. The numbers in squares refer to Lewontin D'×100.
LD = linkage disequilibrium; LOD = logarithm of odds.

Table 4. *ATM*, *PLK2* and *PLK3* haplotypes frequencies in gastric cancer patients and control group

Haplotypes	Total frequency (%)	Frequency		P-value	P_{corr}*
		Controls (%)	Cases (%)		
PLK2					
$C_{rs15009}$-$C_{rs963615}$	0.360	0.402	0.337	**0.022**	**0.050**
$G_{rs15009}$-$C_{rs963615}$	0.349	0.333	0.358	0.389	0.646
$C_{rs15009}$-$T_{rs963615}$	0.285	0.260	0.299	0.144	0.292
PLK3					
$A_{rs17883304}$-$C_{rs12404160}$	0.802	0.791	0.809	0.452	0.883
$C_{rs17883304}$-$T_{rs12404160}$	0.178	0.172	0.183	0.647	0.950
$A_{rs17883304}$-$T_{rs12404160}$	0.018	0.037	0.005	**<0.001**	**0.001**
ATM					
$T_{rs228589}$-$A_{rs189037}$-T_{rs4585}	0.594	0.571	0.609	0.224	0.711
$A_{rs228589}$-$G_{rs189037}$-G_{rs4585}	0.365	0.342	0.379	0.222	0.709
$A_{rs228589}$-$G_{rs189037}$-T_{rs4585}	0.017	0.034	0.005	**<0.001**	**<0.001**
$T_{rs228589}$-$A_{rs189037}$-G_{rs4585}	0.016	0.001	0.041	**<0.001**	**<0.001**

Statistically significant values are highlighted in bold (P<0.05).
*P_{corr}=corrected P-value following the calculation of 10,000 permutations for multiple comparisons.

In silico SNV functional analysis

Next, we performed *in silico* functional analysis of the candidate SNVs with statistically significant associations, including SNVs with observed trends in survival analysis. The 5'-UTR regions and introns typically contain enhancer and silencer regions and bind transcription factors to enhance or repress gene transcription [35,36]. These motifs may also be present in the 3' UTR [37]. Additionally, variations in the 3' UTR may affect the binding of miRs and, therefore, the mRNA expression levels. The results of the disruption of transcription factor binding sites due to polymorphic sites and identification of miRs that differentially bind to these polymorphic sites are summarized in **Table 6**.

In *PLK2* rs963615, a TATA-binding protein (TBP) binding motif was created if the T allele was present. In *PLK2* rs15009 Enkephalin transcription factor 1 (ENKTF-1) appeared to bind in the presence of the C allele, whereas Retinoid X receptor α:Retinoic acid receptor β (RXR-α:RAR-β), Multiprotein bridging factor-1 and vitamin D receptor binding motifs were created when the G allele was present. Moreover, putative binding sites for miR-23a-5p and miR-23b-5p were formed when the G allele of *PLK2* rs15009 was present, in contrast with the C allele. In *PLK3* rs12404160, a binding motif for Purine Rich Box-1 (PU.1) was created in the presence

https://doi.org/10.5230/jgc.2022.22.e31

jgc Journal of Gastric Cancer

Table 5. Associations between *PLK2*, *PLK3*, and *ATM* SNV genotypes and clinicopathological features of patients with GC

Genotypes	Vascular invasion		Perineural invasion	
	OR (95% CI)	P-value	OR (95% CI)	P-value
rs963615 (*PLK2*)				
CC	1 (ref)	0.030	1 (ref)	0.520
CT	0.35 (0.16–0.77)		0.62 (0.26–1.48)	
TT	0.60 (0.18–2.04)		0.62 (0.15–2.59)	
CC:(CT+TT)*	0.39 (0.19–0.83)	0.013	0.62 (0.27–1.41)	0.253
(CC+CT):TT†	0.96 (0.30–3.06)	0.945	0.76 (0.19–3.04)	0.700
(CC+TT):CT‡	0.38 (0.18–0.81)	0.012	0.67 (0.29–1.55)	0.352
rs15009 (*PLK2*)				
CC	1 (ref)	0.314	1 (ref)	0.720
CG	1.39 (0.65–2.95)		1.35 (0.57–3.20)	
GG	2.96 (0.59–4.86)		0.81 (0.16–4.01)	
CC:(CG+GG)*	2.55 (0.75–3.20)	0.239	1.25 (0.55–2.82)	0.598
(CC+CG):GG†	2.55 (0.53–2.33)	0.209	0.72 (0.15–3.39)	0.672
(CC+GG):CG‡	1.21 (0.58–2.53)	0.606	1.39 (0.60–3.21)	0.441
rs17883304 (*PLK3*)				
AA	1 (ref)	0.882	1 (ref)	0.957
AC	0.90 (0.55–1.95)		0.88 (0.37–2.09)	
CC	1.55 (0.15–5.61)		0.94 (0.06–15.66)	
AA:(AC+CC)*	0.94 (0.44–2.00)	0.870	0.88 (0.38–2.06)	0.769
(AA+AC):CC†	1.61 (0.16–5.94)	0.674	0.98 (0.06–16.12)	0.988
(AA+CC):AC‡	0.88 (0.41–1.91)	0.749	0.88 (0.37–2.08)	0.769
rs12404160 (*PLK3*)				
GG	1 (ref)	0.394	1 (ref)	0.828
GA	0.81 (0.37–1.78)		0.91 (0.38–2.16)	
AA	3.16 (0.36–27.55)		1.93 (0.17–22.50)	
GG:(GA+AA)*	0.96 (0.45–2.04)	0.907	0.97 (0.42–2.25)	0.937
(GG+GA):AA†	3.38 (0.39–9.03)	0.208	2.00 (0.18–22.85)	0.566
(GG+AA):GA‡	0.75 (0.34–1.65)	0.482	0.88 (0.37–2.08)	0.769
rs228589 (*ATM*)				
TT	1 (ref)	0.250	1 (ref)	**0.044**
TA	1.15 (0.50–2.63)		0.48 (0.19–1.22)	
AA	0.50 (0.17–1.43)		**0.22 (0.06–0.78)**	
TT:(TA+AA)*	0.92 (0.42–2.00)	0.832	**0.39 (0.16–0.95)**	**0.034**
(TT+TA):AA†	0.46 (0.18–1.16)	0.103	0.34 (0.11–1.05)	0.051
(TT+AA):TA‡	1.47 (0.71–3.05)	0.294	0.81 (0.36–1.83)	0.607
rs189037 (*ATM*)				
AA	1 (ref)	0.237	1 (ref)	**0.044**
AG	1.22 (0.53–2.80)		0.48 (0.19–1.22)	
GG	0.52 (0.18–1.49)		**0.22 (0.06–0.78)**	
AA:(AG+GG)*	0.97 (0.45–2.11)	0.939	**0.39 (0.16–0.95)**	**0.034**
(AA+AG):GG†	1.46 (0.18–1.16)	0.103	0.34 (0.11–1.05)	0.051
(AA+GG):AG‡	1.55 (0.75–3.20)	0.239	0.81 (0.36–1.83)	0.607
rs4585 (*ATM*)				
TT	1 (ref)	0.381	1 (ref)	0.058
TG	1.16 (0.51–2.65)		0.46 (0.18–1.17)	
GG	0.57 (0.20–1.67)		0.24 (0.07–0.86)	
TT:(TG+GG)*	0.97 (0.45–2.11)	0.939	**0.39 (0.16–0.95)**	**0.034**
(TT+TG):GG†	0.52 (0.20–1.34)	0.179	0.38 (0.12–1.19)	0.087
(TT+GG)TG‡	1.41 (0.68–2.92)	0.349	0.74 (0.33–1.67)	0.470

Statistically significant values are highlighted in bold (P<0.05).
SNV = single nucleotide variant; GC = gastric cancer; OR = odds ratio; CI = confidence interval; Ref = reference homozygote.
*Dominant genetic model; †Recessive genetic model; ‡Overdominant genetic model.

of the G allele. In *ATM* rs228589, differential binding motifs for transcription factors Yin yang 1 transcription factor (YY1) and polyoma enhancer activator 3 (PEA3) were formed in the presence of the A allele, whereas in the case of the T allele, the binding motifs for transcription factors glucocorticoid receptor α (GRα), signal transducer and activator of transcription-4,

https://doi.org/10.5230/jgc.2022.22.e31

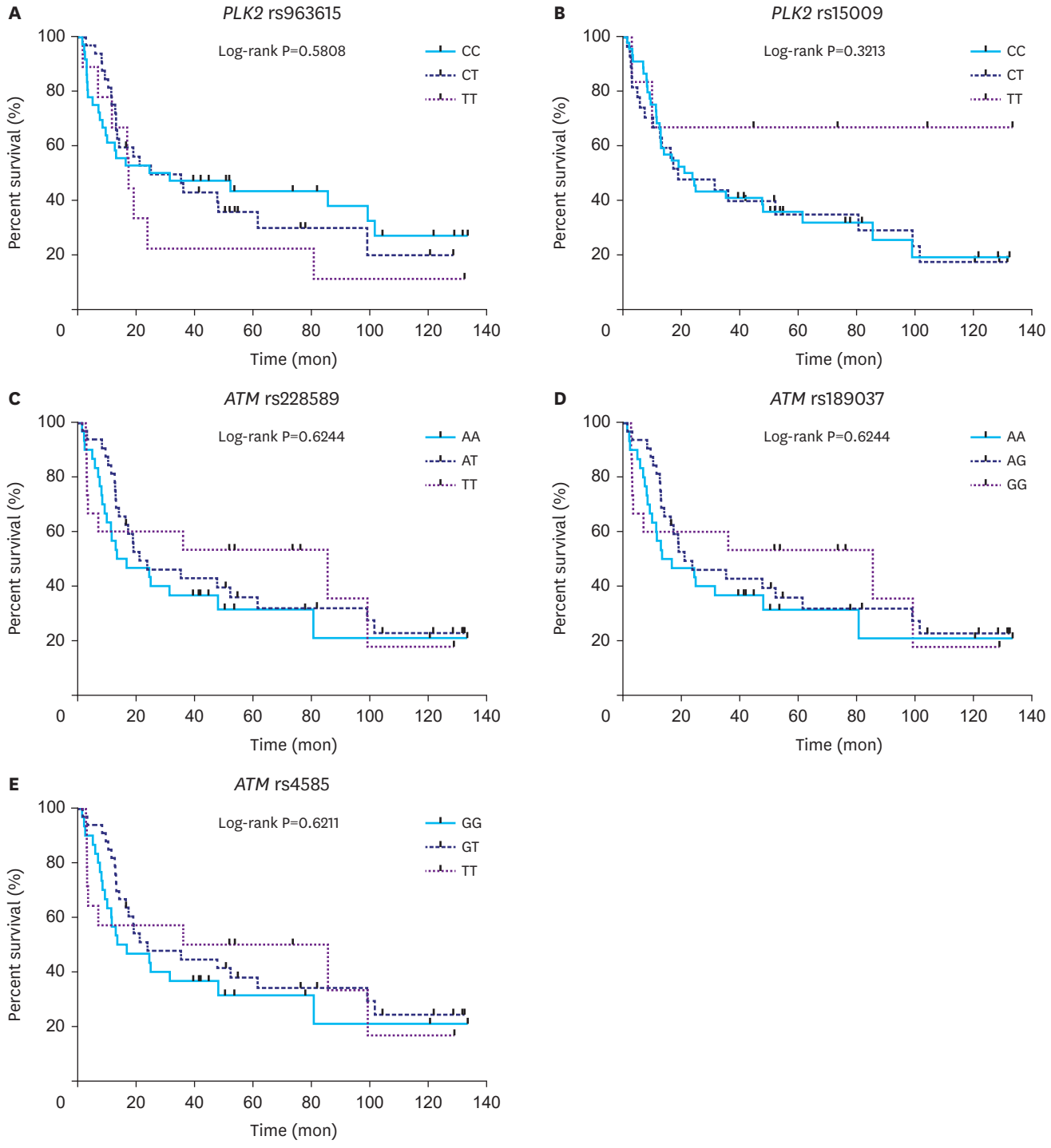

Fig. 2. Survival curves of gastric cancer patients according to the single nucleotide variant genotypes (A) *PLK2* rs963615, (B) *PLK2* rs15009, (C) *ATM* rs228589, (D) *ATM* rs189037 and (E) *ATM* rs4585. Marks indicate censored observations.

c-erythroblast transformation-specific transcription factor-1 (c-Ets-1), and erythroblast transformation-specific Like-1 protein (Elk-1) were generated. In *ATM* rs189037, a binding motif for retinoblastoma-associated protein-1 (E2f-1) is created in the presence of the G allele. Finally, in the presence of the T allele in *ATM* rs4585, binding sites for X-box binding protein-1 (XBP-1) and general transcription factor IID, as well as the binding site for miR-2964a-5p, were created.

https://doi.org/10.5230/jgc.2022.22.e31

jgc Journal of Gastric Cancer

Table 6. Overview of results with significant associations and trends

SNV	Genetic model	Genotype	Association	SNV location	TF binding motifs	miR binding motifs
PLK2						
rs963615	Overdominant	CT	Lower risk in male population	5' UTR	C: / T: TBP	
	Overdominant	CT	Higher risk in female population			
	Overdominant	CT	No vascular invasion			
rs15009*		GG	Higher 10-year survival rate†	3' UTR	C: ENKTF-1, ELK-1 G: RAR-β, RXR-α	C: / G: miR-23a-5p, miR-23b-5p
$C_{rs15009}$-$C_{rs963615}$			Lower risk			
PLK3						
rs12404160	Recessive	AA	Higher risk in male population	Intron	G: PU.1 A: /	
ATM						
rs228589	Dominant	TA+AA	No perineural invasion	Intron	A: YY1, PEA3 T: GR-α, STAT4, c-Ets-1, Elk-1	
rs189037	Dominant	AG+GG	No perineural invasion	5' UTR	A: / G: E2F-1	
rs4585	Dominant	TG+GG	No perineural invasion	3' UTR	T: XBP-1, TFIID G: /	T: miR-2964a-5p G: /
$\mathbf{A}_{rs228589}$-$\mathbf{G}_{rs189037}$-$\mathbf{T}_{rs4585}$			Lower risk			
$\mathbf{T}_{rs228589}$-$\mathbf{A}_{rs189037}$-$\mathbf{G}_{rs4585}$			Higher risk			

Transcription factors and miRs that differentially bind to polymorphic sites are presented in the table.
SNV = single nucleotide variant; TF = transcription factor; miR = micro ribonucleic acid.
*Alleles are reported in the forward orientation; †Observed trend.

miR-23b-5p targets *PLK2* rs15009

Haplotype analysis results suggested that the *PLK2* $\mathbf{C}_{rs15009}$-$\mathbf{C}_{rs963615}$ haplotype may have a marginal protective role in GC risk (P_{corr}=0.050). We performed luciferase reporter assays to evaluate how the presence of different alleles (C/G) in the *PLK2* 3'-UTR region affects the binding of miR-23a-5p and miR-23b-5p, as both have been previously associated with GC [38,39]. The relative luciferase activity of the pmirGLO-PLK2-3'UTR Var (G allele) was decreased by 12% when the cells were co-transfected with the miR-23a-5p mimic (P=0.085) and by 41% when they were co-transfected with the miR-23b-5p mimic (P=0.0097) compared to miR co-transfection in the negative control (**Fig. 3B**). The relative luciferase activity of the pmirGLO-PLK2-3'UTR Wt (C allele) was unaffected by co-transfection with both mimics (**Fig. 3B**). These results suggest that miR-23b-5p directly targets *PLK2* when the G allele is present in *PLK2* rs15009.

We used the KM plotter online tool to analyze whether miR-23b-5p could have prognostic value in patients with GC (**Fig. 3C**). The analysis showed that low miR-23b-5p expression predicted longer 10-year survival in patients with GC (hazard ratio=1.52, P=0.0066). There was no significant correlation between miR-23a-5p expression and overall survival in GC patients using the KM plotter tool (P=0.304, data not shown). We also analyzed differential miR-23b-5p expression in the TCGA_STAD (The Cancer Genome Atlas Stomach Adenocarcinoma) dataset as well as available GEO datasets to evaluate miR-23b-5p expression in tumor vs. normal or high-grade vs. low-grade samples: the results are shown in **Fig. 3D and E**. MiR-23b-5p was downregulated (log FC=-1.26) in tumor sample compared to normal samples (TCGA_STAD dataset, $P_{adj} = 4.88\times10^{-3}$) (**Fig. 3D**). Notably, in the GSE33743 dataset, miR-23b-5p was upregulated in tumors compared to normal samples (log FC=0.76, $P_{adj}=3.21\times10^{-2}$). MiR-23b-5p expression was downregulated in high grade vs. low grade tumour samples from the TCGA_STAD dataset (**Fig. 3E**): in grade 2 vs. grade 1, log FC was −1.93 ($P_{adj}=2.98\times10^{-16}$); in grade 3 vs. grade 1, log FC was −2.54 ($P_{adj}=2.52\times10^{-24}$); in grade 4 vs. grade 1, log FC was −0.64 ($P_{adj} = 2.67\ x10^{-2}$); in grade 4 vs. grade 2, log FC was −0.61 ($P_{adj}=4.02\times10^{-}$

https://doi.org/10.5230/jgc.2022.22.e31

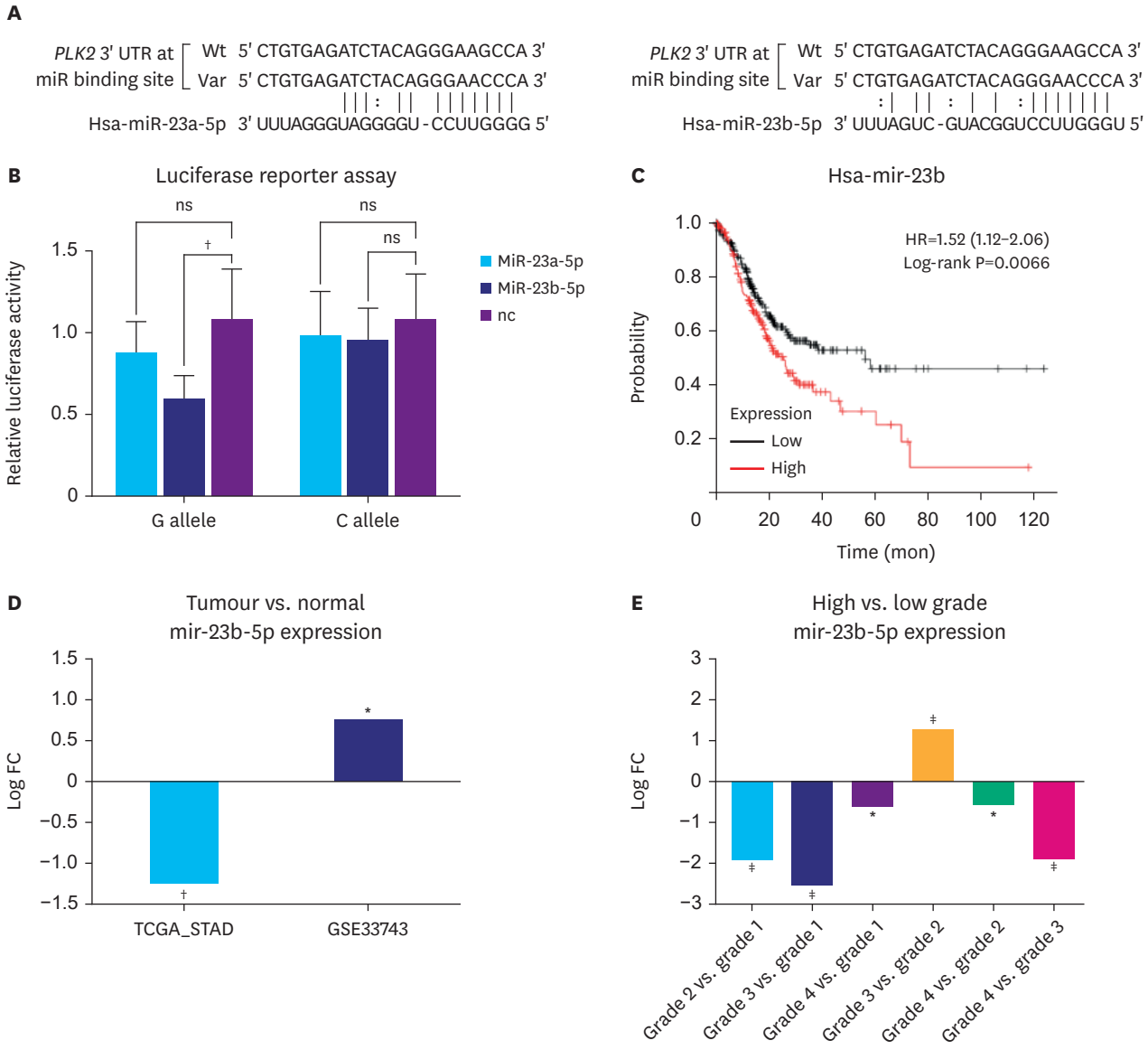

Fig. 3. miR-23b-5p directly targets the G allele in *PLK2* rs15009. (A) Hsa-miR-23a-5p (left) and hsa-miR-23b-5p (right) sequences and *PLK2* 3′ UTRs at miR binding sites (reverse strand sequence). Polymorphic alleles are highlighted in bold. Wt and Var alleles are presented. (B) Relative luciferase activity of the pmirGLO-PLK2-3'UTR Var (G allele) was significantly decreased (P=0.0097) when the miR-23b-5p mimic was co-transfected into the MKN45 cell line, while it was unaffected by miR-23a-5p mimic co-transfection (P=0.0875). Relative luciferase activities of the pmirGLO-PLK2-3'UTR Wt (C allele) were unaffected by co-transfection with miR-23a-5p and miR-23b-5p mimics. Alleles are reported in the forward orientation. (C) Kaplan–Meier survival curves evaluating the overall survival of patients with stomach adenocarcinoma in the TCGA dataset (n=436), based on the expression of miR-23b, using the KM Plotter online tool. (D) Differential miR-23b-5p expression analysis from the TCGA_STAD (case=436, control=41) and GSE33743 datasets (case=37, control=4) in tumour vs. normal samples. (E) Differential miR-23b-5p expression analysis from TCGA_STAD dataset in high vs. low grade samples (grade 1=58, grade 2=128, grade 3=180, grade 4=43).
UTR = untranslated region; miR = micro RNA; Wt = wild-type allele; Var = variant allele; ns = not significant; nc = negative control miR; HR = hazard ratio; FC = fold change; TCGA = The Cancer Genome Atlas.
*P≤0.05; †P≤0.01; ‡P≤0.0001.

[3]); and in grade 4 vs. grade 3, log FC was −1.90 (P_{adj}=4.89×10^{-23}). Mir-23b-5p expression was upregulated when comparing grade 3 vs. grade 2 TCGA_STAD datasets, where log FC was 1.29 (P_{adj}=2.26×10^{-13}) (**Fig. 3E**).

https://doi.org/10.5230/jgc.2022.22.e31

jgc Journal of Gastric Cancer

DISCUSSION

In this study, we investigated the associations between SNVs in cell cycle genes, *PLK2*, *PLK3*, and *ATM,* and GC risk and the clinicopathological features of patients with GC. Candidate SNVs with significant associations were further functionally analyzed to determine their potential regulatory effects on transcription factors and miRNA-binding sites. We also confirmed the putative *PLK2* binding site for miR-23b-5p *in vitro*.

GC is approximately twice as likely to be diagnosed in men than in women [1]. Incidence variation by sex has been attributed to sex-specific lifestyles and potential underlying hormonal mechanisms. The *PLK2* rs963615 CT genotype could be used for selection of female persons at higher GC risk and as a determinant for lower GC risk in the male population. In the presence of the T allele, a binding motif for the transcription factor, TBP, was formed according to *in silico* functional analysis. The expression level of TBP has been confirmed to affect cell proliferation and transformation potential [40]. Additional sex-specific cellular factors may also contribute to TBP levels. Next, the *PLK3* rs12404160 AA genotype could be used as a biomarker for the selection of male individuals at higher GC risk. *In silico* functional analysis implied a binding motif for the transcription factor, PU.1, in the presence of the G allele, suggesting that PU.1 may increase *PLK3* transcriptional activity, which may result in tumor suppression. PU.1 has been previously identified as a tumor suppressor or oncogene in different types of leukemias, breast cancers [41], and gliomas [42]. PU.1 inhibition by small-molecule inhibitors or RNA interference decreases the tumor burden and increased the survival of patients with acute myeloid leukemia [43]. Further studies are necessary to confirm how PU.1 affects *PLK3* transcription, how PU.1-associated actions differ in male and female patients, and whether it would be beneficial to inhibit or promote its activity in patients with GC.

Haplotype analysis results suggest that the *PLK2* $\mathbf{C}_{rs15009}$-$\mathbf{C}_{rs963615}$ haplotype may have a protective role against GC, although the significance was borderline. To our knowledge, *PLK2* rs15009, which lies in the 3' UTR region of the gene, has been studied only in association with the Reelin signaling pathway in Alzheimer's disease, where the authors showed that CC and GG genotypes had a protective effect [44]. *In silico* analysis results for *PLK2* rs15009 suggested that binding of RXR-α and RAR-β proteins in the presence of the G allele and binding of ELK-1 and ENKTF-1 in the presence of the C allele may alter the level of *PLK2* expression. RXR-α and RAR-β are retinoic acid nuclear receptors that regulate apoptosis, cell cycle, and differentiation [45]. Lower RXR-α expression has been reported in patients with GC and is significantly associated with advanced disease stages [46]. RAR-β hypermethylation is predominantly associated with diffuse GC [44]. Notably, in this study, it was further established that RAR-β methylation status was statistically associated with invasion, differentiation, and location of the tumor in diffuse types, whereas these histopathological features were not associated with RAR-β methylation status in intestinal types of GC [47]. This indicates that different levels of DNA binding factors or their differential binding to polymorphic sites could profoundly affect their downstream pathways and, thus, influence the development of distinct tumor types. Similarly, it has been found that ELK-1 activity promotes cell migration and invasion and is involved in cancer development due to inflammation [48,49]. Therefore, aberrant ELK-1 activity due to SNVs can affect *PLK2* transcription and mRNA-associated processes.

https://doi.org/10.5230/jgc.2022.22.e31

jgc Journal of Gastric Cancer

Using a luciferase reporter assay, we analyzed the binding of miR-23a-5p and miR-23b-5p to *PLK2* rs15009, which was selected as the best potential binding candidate for *in silico* analysis. We confirmed that miR-23b-5p binds specifically to the *PLK2* rs15009 G allele. It has been proposed that miR-23b plays a dichotomous role in cancer, either as a tumor suppressor or as an oncogene. MiR-23b expression is downregulated in human glioma, prostate, bladder, breast, and gastrointestinal cancers and has been shown to suppress tumor growth, invasion, angiogenesis, and metastasis and affect chemoresistance and tumor cell dormancy [50-55]. In contrast, some studies have shown that the expression of miR-23b is upregulated, and that it may also function as an oncogene by promoting tumor growth, proliferation, and metastasis in prostate and breast cancer, as well as in GC [56-58]. Analysis of paired tumor-normal samples from 160 gastric adenocarcinoma patients demonstrated that co-expression of miR-23a and miR-23b was significantly upregulated, particularly in specimens from patients at advanced stages (II-IV), and correlated with lymph node metastasis [38]. In addition, miR-23a/b enhanced tumor growth in a GC xenograft mouse model by inhibiting apoptosis of GC cells by directly targeting a tumor suppressor, programmed cell death 4 protein. The observed function of miR-23b as an oncomir is in line with our survival analysis results using the KM plotter on GC samples from the TCGA database. Lower miR-23b expression was associated with a higher 10-year survival rate. These results suggest that miR-23b-5p may serve as a prognostic factor for tumor progression and survival. Significantly shorter 5-year overall survival and disease-free survival were observed in patients with higher plasma miR-23b expression [59].

Notably, public dataset expression analysis showed that miR-23b-5p was downregulated in the TCGA_STAD cohort and upregulated in the GSE33743 cohort. It is worth noting that the first cohort included 436 tumor and 41 normal samples in the analysis, whereas the latter only analyzed 37 tumor and four normal samples. When comparing expression in high-vs. low-grade samples, miR-23b-5p was mostly downregulated, with the exception of the grade 3 vs. grade 2 comparison, where it was upregulated. These results suggest that miR-23b-5p may serve as a prognostic factor for tumor progression. Low miR-23b-5p expression appears to be associated with greater overall survival. Furthermore, comparison of its expression in high-and low-grade tumor tissues indicated that its expression could gradually decrease during tumor progression. This confirmed the dichotomous role of miR-23b, as discussed above. For better interpretation, analysis of samples grouped by sex, clinical and histological parameters, whether therapy is administered, and outcome, is necessary. Overall, the perplexing behavior of miRs confirms that in complex and heterogenic diseases such as GC, it is necessary to develop systems medicine approaches to decipher oncogenic mechanisms.

Therefore, the protective role of the *PLK2* $\mathbf{C}_{rs15009}$-$\mathbf{C}_{rs963615}$ haplotype in GC could be explained by *PLK2* repression through miR-23b-5p binding to the G allele. To draw more definite conclusions from our study, we wanted to analyze a cohort in which the *PLK2* rs15009 genotype, miR-23b-5p expression, and *PLK2* mRNA expression would be known, possibly together with data on patient survival or response to therapy. Unfortunately, we were unable to obtain such datasets from publicly available databases. Nevertheless, we can theoretically consider two scenarios in which data on *PLK2* rs15009 and miR-23b-5p expression levels would have clinical value. In the first scenario, individuals with the risk *PLK2* rs15009 haplotype would also have overexpression of miR-23b-5p. This combination could result in the decreased expression and functional activity of PLK2 during the cell cycle. This would lead to tumor progression since PLK2 acts as a tumor suppressor [10-12]. In the second scenario, individuals with the *PLK2* risk haplotype, who have miR-23b-5p underexpression,

https://doi.org/10.5230/jgc.2022.22.e31

jgc Journal of Gastric Cancer

would have *PLK2* mRNA levels higher than usual. High PLK2 levels are associated with a protective role in cancer, but might also lead to chemoresistance in individuals receiving chemotherapy. Previous observations have shown that at higher expression levels, PLK2 significantly predicted a poorer outcome in patients with colorectal cancer by enhancing chemoresistance [60]. PLK2 has also been proposed to be an important determinant of chemotherapy sensitivity in ovarian cancer [61]. Its repression through miR-23b-5p in the presence of the rs15009 G allele could reduce chemoresistance. Therefore, depending on the disease grade and whether therapy is administered, *PLK2* rs15009 could be useful as a biomarker of chemotherapy resistance prediction in GC in combination with miR-23b expression levels. This could be exploited in the future for the development of novel targeted PLK2 therapies using either miR or PLK2 inhibitors or miR mimics [62]. Interactions between other proteins and miRNAs should also be considered.

The *PLK2* rs963615 CT genotype was significantly associated with the absence of vascular invasion, whereas *ATM* rs228589, rs189037, and rs4585 were significantly associated with the absence of perineural invasion. These SNVs could be used in clinical settings to aid in prognosis and possibly in the determination of the most suitable treatment options for patients. The A allele of *ATM* rs228589 has been previously associated with a higher risk of chronic myeloid leukemia in the Indian population [63], whereas the T allele has been associated with a higher risk of breast cancer in the Jewish female population [64]. In a meta-analysis conducted by Zhao et al., the A allele in *ATM* rs189037 was significantly associated with breast, oral, and lung cancer risk in East Asian and Latino populations, but not in Caucasians [65]. Moreover, the AA genotype of rs189037 is significantly associated with a higher GC risk in the Chinese population [66]. It was also associated with higher TNM stage, overall tumor size, and survival prognosis. This is in concordance with our results, where *ATM* rs189037 AG + GG genotypes were associated with the absence of perineural invasion. *ATM* SNV rs4585 is associated with a lower risk of papillary thyroid carcinoma in the *ATM* haplotype, $C_{rs373759}$-$G_{rs664143}$-T_{rs4585} [67]. Notably, our results indicated that the *ATM* haplotype, $T_{rs228589}$-$A_{rs189037}$-$G_{rs4585,}$ was significantly more frequent, whereas $A_{rs228589}$-$G_{rs189037}$-T_{rs4585} was significantly reduced in patients with GC. The differences in associations between specific alleles and cancer risk may be due to the different ethnicities of the studied populations and different cancer types.

In silico analysis resulted in several transcription factor candidates that may, through *ATM* activation or silencing, depending on specific allele binding, contribute to higher GC risk (haplotype analysis) or the absence of perineural invasion. Low ATM expression is generally associated with more aggressive tumors. In contrast, overexpression of ATM may lead to cisplatin resistance, resulting in a less favorable prognosis [68]. The A allele of *ATM* rs228589 forms a binding site for YY1 and PEA3; however, this binding motif is lost if an individual is a carrier of the T allele. YY1 expression is upregulated in GC cell lines and tissues, contributing to gastric carcinogenesis [69]. YY1 is also considered a potential therapeutic target [70]. PEA3 was upregulated in gastric adenocarcinoma samples, and together with the ERK signaling pathway, indicated poor survival prognosis [71]. In the presence of the G allele of *ATM* rs189037, a binding motif for E2f-1 is formed. E2f-1 has been previously associated with poor overall survival in GC [72]. However, E2f-1 overexpression in the MGC-803 GC cell line results in cell growth and proliferation inhibition, reduced invasion, and a higher apoptotic rate [73]. When the G allele is present, a binding site for STAT-4 and c-Ets-1 is formed. High STAT expression has been associated with better clinical outcomes in GC [74]. C-Ets-1 expression is correlated with *H. pylori* infection, a major risk factor for GC [75]. The T allele of *ATM* rs4585

https://doi.org/10.5230/jgc.2022.22.e31

jgc Journal of Gastric Cancer

participates in the formation of a binding motif for XBP-1. XBP-1 is involved in endoplasmic reticulum stress and unfolded protein response and it generally promotes cancer cell survival and tumor progression [76]. XBP-1 is a crucial factor that promotes tumor growth and invasion in GC while inhibiting apoptosis and autophagy [77]. Additionally, the hsa-miR-29641-5p binding site is formed in the presence of the T allele. Binding has been confirmed *in vitro*, and results in decreased *ATM* expression [78]. MiR-29641-5p has been characterized as an oncomiR in periampullary adenocarcinoma [79] and breast cancer [80].

Histological type, degree of differentiation, and molecular type of the tumor, as well as genetic background and cooperation between multiple miRs and miRNA-transcription factors may affect the final role of particular miR on gene expression. There are a few limitations to the power of SNV association studies. In complex diseases, the contribution of a particular SNV is usually modest. Study population size, allele frequencies, LD, and other parameters affect the power of the study [81]. We performed a candidate gene association study, which is a targeted approach compared to genome-wide association studies, where screening is untargeted and associations for marker SNVs are studied. Candidate gene association studies enhance the power of the study and are important when studying low-frequency SNVs or when the study population is small, as in our case. Our study included 221 patients with GC and 321 healthy controls. In small study populations, larger effects are easier to detect, whereas smaller effects might be missed, leading to false negatives. Another limiting factor is the minimum MAF, which is typically 0.05 [82]. To compensate for the small sample size, we selected SNPs with MAFs≥0.10. Enriching for more common alleles increases the power to detect associations. However, it is important to keep in mind that rarer SNVs may have larger effect sizes, and omitting them may be potentially counterproductive [83]. Moreover, we assessed the MAF in our study group and CEU to ensure that they were comparable. When performing the analyses of risk-associated haplotypes, we included adjustments for multiple comparisons to avoid false positives. In some cases, the sample sizes were small for association tests between SNVs and clinicopathological features. Unfortunately, clinical data were not available for all the patients. Additionally, some reported associations are marginal; therefore, our results should be interpreted with caution and further validated in a larger cohort.

Our study indicates a possible role for *PLK2*, *PLK3*, and *ATM* SNVs in gastric tumorigenesis. We also show that *PLK2* is targeted by miR-23b-5p *in vitro* and that low expression of miR-23b-5p in tumors is associated with better survival prognosis. Analyses of inter-individual genetic variability are of paramount importance in precision medicine, as they can significantly influence occurrence, course, and response to treatment. Low-penetrating variations in cell cycle genes may affect transcription factor and miR binding and can serve as biomarkers for tailored therapy selection, such as small-molecule or RNA inhibitors of transcription factors or oncomiR inhibitors. The current understanding of the molecular etiology and progression of GC is limited, and there is a critical need to explore novel genetic and molecular candidates that might contribute to the better management of this multifaceted disease.

ACKNOWLEDGMENTS

We express our gratitude to Dubravka Germ and Urša Adamič for their technical assistance with DNA isolation.

https://doi.org/10.5230/jgc.2022.22.e31

jgc Journal of Gastric Cancer

SUPPLEMENTARY MATERIALS

Supplementary Table 1

Genotype frequencies distributions and HWE for candidate SNVs among control population and gastric cancer patients

Click here to view

Supplementary Table 2

Associations between *PLK2*, *PLK3*, and *ATM* SNV genotypes and clinicopathological features of GC patients

Click here to view

Supplementary Fig. 1

Minor genotype (A) and allele (B) frequencies for SNVs rs963615 (PLK2), rs15009 (PLK2), rs17883304 (PLK3), rs12404160 (PLK3), rs228589 (ATM), rs189037 (ATM), rs4585 (ATM) in populations.

Click here to view

REFERENCES

1. Sung H, Ferlay J, Siegel RL, Laversanne M, Soerjomataram I, Jemal A, et al. Global cancer statistics 2020: GLOBOCAN estimates of incidence and mortality worldwide for 36 cancers in 185 countries. CA Cancer J Clin 2021;71:209-249.
PUBMED | CROSSREF
2. Oliveira C, Pinheiro H, Figueiredo J, Seruca R, Carneiro F. Familial gastric cancer: genetic susceptibility, pathology, and implications for management. Lancet Oncol 2015;16:e60-e70.
PUBMED | CROSSREF
3. Cancer Genome Atlas Research Network. Comprehensive molecular characterization of gastric adenocarcinoma. Nature 2014;513:202-209.
PUBMED | CROSSREF
4. Maleki SS, Röcken C. Chromosomal instability in gastric cancer biology. Neoplasia 2017;19:412-420.
PUBMED | CROSSREF
5. Bakhoum SF, Silkworth WT, Nardi IK, Nicholson JM, Compton DA, Cimini D. The mitotic origin of chromosomal instability. Curr Biol 2014;24:R148-R149.
PUBMED | CROSSREF
6. Burrell RA, McClelland SE, Endesfelder D, Groth P, Weller MC, Shaikh N, et al. Replication stress links structural and numerical cancer chromosomal instability. Nature 2013;494:492-496.
PUBMED | CROSSREF
7. Gao L, Nieters A, Brenner H. Cell proliferation-related genetic polymorphisms and gastric cancer risk: systematic review and meta-analysis. Eur J Hum Genet 2009;17:1658-1667.
PUBMED | CROSSREF
8. Jiang N, Wang X, Jhanwar-Uniyal M, Darzynkiewicz Z, Dai W. Polo box domain of Plk3 functions as a centrosome localization signal, overexpression of which causes mitotic arrest, cytokinesis defects, and apoptosis. J Biol Chem 2006;281:10577-10582.
PUBMED | CROSSREF
9. Burns TF, Fei P, Scata KA, Dicker DT, El-Deiry WS. Silencing of the novel p53 target gene Snk/Plk2 leads to mitotic catastrophe in paclitaxel (taxol)-exposed cells. Mol Cell Biol 2003;23:5556-5571.
PUBMED | CROSSREF
10. Syed N, Smith P, Sullivan A, Spender LC, Dyer M, Karran L, et al. Transcriptional silencing of Polo-like kinase 2 (SNK/PLK2) is a frequent event in B-cell malignancies. Blood 2006;107:250-256.
PUBMED | CROSSREF

11. Benetatos L, Dasoula A, Hatzimichael E, Syed N, Voukelatou M, Dranitsaris G, et al. Polo-like kinase 2 (SNK/PLK2) is a novel epigenetically regulated gene in acute myeloid leukemia and myelodysplastic syndromes: genetic and epigenetic interactions. Ann Hematol 2011;90:1037-1045.
PUBMED | CROSSREF
12. Pellegrino R, Calvisi DF, Ladu S, Ehemann V, Staniscia T, Evert M, et al. Oncogenic and tumor suppressive roles of polo-like kinases in human hepatocellular carcinoma. Hepatology 2010;51:857-868.
PUBMED | CROSSREF
13. Chichirau BE, Scheidt T, Diechler S, Neuper T, Horejs-Hoeck J, Huber CG, et al. Dissecting the *Helicobacter pylori*-regulated transcriptome of B cells. Pathog Dis 2020;78:ftaa049.
PUBMED | CROSSREF
14. Li B, Ouyang B, Pan H, Reissmann PT, Slamon DJ, Arceci R, et al. Prk, a cytokine-inducible human protein serine/threonine kinase whose expression appears to be down-regulated in lung carcinomas. J Biol Chem 1996;271:19402-19408.
PUBMED | CROSSREF
15. Dai W, Li Y, Ouyang B, Pan H, Reissmann P, Li J, et al. PRK, a cell cycle gene localized to 8p21, is downregulated in head and neck cancer. Genes Chromosomes Cancer 2000;27:332-336.
PUBMED | CROSSREF
16. Dai W, Liu T, Wang Q, Rao CV, Reddy BS. Down-regulation of PLK3 gene expression by types and amount of dietary fat in rat colon tumors. Int J Oncol 2002;20:121-126.
PUBMED | CROSSREF
17. Abraham RT. Cell cycle checkpoint signaling through the ATM and ATR kinases. Genes Dev 2001;15:2177-2196.
PUBMED | CROSSREF
18. Giunta S, Belotserkovskaya R, Jackson SP. DNA damage signaling in response to double-strand breaks during mitosis. J Cell Biol 2010;190:197-207.
PUBMED | CROSSREF
19. Suarez F, Mahlaoui N, Canioni D, Andriamanga C, Dubois d'Enghien C, Brousse N, et al. Incidence, presentation, and prognosis of malignancies in ataxia-telangiectasia: a report from the French national registry of primary immune deficiencies. J Clin Oncol 2015;33:202-208.
PUBMED | CROSSREF
20. Helgason H, Rafnar T, Olafsdottir HS, Jonasson JG, Sigurdsson A, Stacey SN, et al. Loss-of-function variants in ATM confer risk of gastric cancer. Nat Genet 2015;47:906-910.
PUBMED | CROSSREF
21. Xu Z, Taylor JA. SNPinfo: integrating GWAS and candidate gene information into functional SNP selection for genetic association studies. Nucleic Acids Res 2009;37:W600-5.
PUBMED | CROSSREF
22. Barrett JC. Haploview: visualization and analysis of SNP genotype data. Cold Spring Harb Protoc 2009;2009:pdb.ip71.
PUBMED | CROSSREF
23. Chen B, Wilkening S, Drechsel M, Hemminki K. SNP_tools: a compact tool package for analysis and conversion of genotype data for MS-Excel. BMC Res Notes 2009;2:214.
PUBMED | CROSSREF
24. Ruiz-Larrañaga O, Garrido JM, Iriondo M, Manzano C, Molina E, Koets AP, et al. Genetic association between bovine NOD2 polymorphisms and infection by *Mycobacterium avium* subsp. *paratuberculosis* in Holstein-Friesian cattle. Anim Genet 2010;41:652-655.
PUBMED | CROSSREF
25. Farré D, Roset R, Huerta M, Adsuara JE, Roselló L, Albà MM, et al. Identification of patterns in biological sequences at the ALGGEN server: PROMO and MALGEN. Nucleic Acids Res 2003;31:3651-3653.
PUBMED | CROSSREF
26. Messeguer X, Escudero R, Farré D, Núñez O, Martínez J, Albà MM. PROMO: detection of known transcription regulatory elements using species-tailored searches. Bioinformatics 2002;18:333-334.
PUBMED | CROSSREF
27. Liu C, Zhang F, Li T, Lu M, Wang L, Yue W, et al. MirSNP, a database of polymorphisms altering miRNA target sites, identifies miRNA-related SNPs in GWAS SNPs and eQTLs. BMC Genomics 2012;13:661.
PUBMED | CROSSREF
28. Riolo G, Cantara S, Marzocchi C, Ricci C. miRNA targets: from prediction tools to experimental validation. Methods Protoc 2020;4:1.
PUBMED | CROSSREF
29. Aken BL, Achuthan P, Akanni W, Amode MR, Bernsdorff F, Bhai J, et al. Ensembl 2017. Nucleic Acids Res 2017;45:D635-D642.
PUBMED | CROSSREF

30. Team R. RStudio: Integrated Development Environment for R. Boston (MA): RStudio, Inc., 2016.
31. González JR, Armengol L, Solé X, Guinó E, Mercader JM, Estivill X, et al. SNPassoc: an R package to perform whole genome association studies. Bioinformatics 2007;23:644-645.
PUBMED | CROSSREF
32. Vrieze SI. Model selection and psychological theory: a discussion of the differences between the Akaike information criterion (AIC) and the Bayesian information criterion (BIC). Psychol Methods 2012;17:228-243.
PUBMED | CROSSREF
33. Nagy Á, Munkácsy G, Győrffy B. Pancancer survival analysis of cancer hallmark genes. Sci Rep 2021;11:6047.
PUBMED | CROSSREF
34. Xu F, Wang Y, Ling Y, Zhou C, Wang H, Teschendorff AE, et al. dbDEMC 3.0: Functional exploration of differentially expressed miRNAs in cancers of human and model organisms. Genomics Proteomics Bioinformatics 2022;S1672-0229(22)00068-7.
PUBMED | CROSSREF
35. Jash A, Yun K, Sahoo A, So JS, Im SH. Looping mediated interaction between the promoter and 3′ UTR regulates type II collagen expression in chondrocytes. PLoS One 2012;7:e40828.
PUBMED | CROSSREF
36. Degtyareva AO, Antontseva EV, Merkulova TI. Regulatory SNPs: altered transcription factor binding sites implicated in complex traits and diseases. Int J Mol Sci 2021;22:6454.
PUBMED | CROSSREF
37. Steri M, Idda ML, Whalen MB, Orrù V. Genetic variants in mRNA untranslated regions. Wiley Interdiscip Rev RNA 2018;9:e1474.
PUBMED | CROSSREF
38. Ma G, Dai W, Sang A, Yang X, Gao C. Upregulation of microRNA-23a/b promotes tumor progression and confers poor prognosis in patients with gastric cancer. Int J Clin Exp Pathol 2014;7:8833-8840.
PUBMED
39. Hu X, Wang Y, Liang H, Fan Q, Zhu R, Cui J, et al. miR-23a/b promote tumor growth and suppress apoptosis by targeting PDCD4 in gastric cancer. Cell Death Dis 2017;8:e3059.
PUBMED | CROSSREF
40. Johnson SA, Dubeau L, White RJ, Johnson DL. The TATA-binding protein as a regulator of cellular transformation. Cell Cycle 2003;2:442-444.
PUBMED | CROSSREF
41. Lin J, Liu W, Luan T, Yuan L, Jiang W, Cai H, et al. High expression of PU.1 is associated with Her-2 and shorter survival in patients with breast cancer. Oncol Lett 2017;14:8220-8226.
PUBMED | CROSSREF
42. Xu Y, Gu S, Bi Y, Qi X, Yan Y, Lou M. Transcription factor PU.1 is involved in the progression of glioma. Oncol Lett 2018;15:3753-3759.
PUBMED | CROSSREF
43. Antony-Debré I, Paul A, Leite J, Mitchell K, Kim HM, Carvajal LA, et al. Pharmacological inhibition of the transcription factor PU.1 in leukemia. J Clin Invest 2017;127:4297-4313.
PUBMED | CROSSREF
44. Bufill E, Roura-Poch P, Sala-Matavera I, Antón S, Lleó A, Sánchez-Saudinós B, et al. Reelin signaling pathway genotypes and Alzheimer disease in a Spanish population. Alzheimer Dis Assoc Disord 2015;29:169-172.
PUBMED | CROSSREF
45. Balmer JE, Blomhoff R. Gene expression regulation by retinoic acid. J Lipid Res 2002;43:1773-1808.
PUBMED | CROSSREF
46. Hu KW, Chen FH, Ge JF, Cao LY, Li H. Retinoid receptors in gastric cancer: expression and influence on prognosis. Asian Pac J Cancer Prev 2012;13:1809-1817.
PUBMED | CROSSREF
47. Mohsenzadeh M, Sadeghi RN, Vahedi M, Kamani F, Hashemi M, Asadzadeh H, et al. Promoter hypermethylation of RAR-β tumor suppressor gene in gastric carcinoma: Association with histological type and clinical outcomes. Cancer Biomark 2017;20:7-15.
PUBMED | CROSSREF
48. Odrowaz Z, Sharrocks AD. The ETS transcription factors ELK1 and GABPA regulate different gene networks to control MCF10A breast epithelial cell migration. PLoS One 2012;7:e49892.
PUBMED | CROSSREF
49. Kasza A. IL-1 and EGF regulate expression of genes important in inflammation and cancer. Cytokine 2013;62:22-33.
PUBMED | CROSSREF

50. Majid S, Dar AA, Saini S, Arora S, Shahryari V, Zaman MS, et al. miR-23b represses proto-oncogene Src kinase and functions as methylation-silenced tumor suppressor with diagnostic and prognostic significance in prostate cancer. Cancer Res 2012;72:6435-6446.
PUBMED | CROSSREF
51. Majid S, Dar AA, Saini S, Deng G, Chang I, Greene K, et al. MicroRNA-23b functions as a tumor suppressor by regulating Zeb1 in bladder cancer. PLoS One 2013;8:e67686.
PUBMED | CROSSREF
52. Ono M, Kosaka N, Tominaga N, Yoshioka Y, Takeshita F, Takahashi RU, et al. Exosomes from bone marrow mesenchymal stem cells contain a microRNA that promotes dormancy in metastatic breast cancer cells. Sci Signal 2014;7:ra63.
PUBMED | CROSSREF
53. An Y, Zhang Z, Shang Y, Jiang X, Dong J, Yu P, et al. miR-23b-3p regulates the chemoresistance of gastric cancer cells by targeting ATG12 and HMGB2. Cell Death Dis 2015;6:e1766.
PUBMED | CROSSREF
54. Geng J, Luo H, Pu Y, Zhou Z, Wu X, Xu W, et al. Methylation mediated silencing of miR-23b expression and its role in glioma stem cells. Neurosci Lett 2012;528:185-189.
PUBMED | CROSSREF
55. Zhang H, Hao Y, Yang J, Zhou Y, Li J, Yin S, et al. Genome-wide functional screening of miR-23b as a pleiotropic modulator suppressing cancer metastasis. Nat Commun 2011;2:554.
PUBMED | CROSSREF
56. Tian L, Fang YX, Xue JL, Chen JZ. Four microRNAs promote prostate cell proliferation with regulation of PTEN and its downstream signals in vitro. PLoS One 2013;8:e75885.
PUBMED | CROSSREF
57. Jin L, Wessely O, Marcusson EG, Ivan C, Calin GA, Alahari SK. Prooncogenic factors miR-23b and miR-27b are regulated by Her2/Neu, EGF, and TNF-α in breast cancer. Cancer Res 2013;73:2884-2896.
PUBMED | CROSSREF
58. Qi P, Xu MD, Shen XH, Ni SJ, Huang D, Tan C, et al. Reciprocal repression between TUSC7 and miR-23b in gastric cancer. Int J Cancer 2015;137:1269-1278.
PUBMED | CROSSREF
59. Zhuang K, Han K, Tang H, Yin X, Zhang J, Zhang X, et al. Up-regulation of plasma miR-23b is associated with poor prognosis of gastric cancer. Med Sci Monit 2016;22:356-361.
PUBMED | CROSSREF
60. Xie Y, Liu Y, Li Q, Chen J. Polo-like kinase 2 promotes chemoresistance and predicts limited survival benefit from adjuvant chemotherapy in colorectal cancer. Int J Oncol 2018;52:1401-1414.
PUBMED | CROSSREF
61. Coley HM, Hatzimichael E, Blagden S, McNeish I, Thompson A, Crook T, et al. Polo Like Kinase 2 Tumour Suppressor and cancer biomarker: new perspectives on drug sensitivity/resistance in ovarian cancer. Oncotarget 2012;3:78-83.
PUBMED | CROSSREF
62. Korns J, Liu X, Takiar V. A review of Plks: thinking outside the (polo) box. Mol Carcinog 2022;61:254-263.
PUBMED | CROSSREF
63. Gorre M, Mohandas PE, Kagita S, Cingeetham A, Vuree S, Jarjapu S, et al. Significance of ATM gene polymorphisms in chronic myeloid leukemia - a case control study from India. Asian Pac J Cancer Prev 2016;17:815-821.
PUBMED | CROSSREF
64. Koren M, Kimmel G, Ben-Asher E, Gal I, Papa MZ, Beckmann JS, et al. ATM haplotypes and breast cancer risk in Jewish high-risk women. Br J Cancer 2006;94:1537-1543.
PUBMED | CROSSREF
65. Zhao ZL, Xia L, Zhao C, Yao J. ATM rs189037 (G > A) polymorphism increased the risk of cancer: an updated meta-analysis. BMC Med Genet 2019;20:28.
PUBMED | CROSSREF
66. Tao Y, Mei Y, Ying R, Chen S, Wei Z. The ATM rs189037 G>A polymorphism is associated with the risk and prognosis of gastric cancer in Chinese individuals: a case-control study. Gene 2020;741:144578.
PUBMED | CROSSREF
67. Song CM, Kwon TK, Park BL, Ji YB, Tae K. Single nucleotide polymorphisms of ataxia telangiectasia mutated and the risk of papillary thyroid carcinoma. Environ Mol Mutagen 2015;56:70-76.
PUBMED | CROSSREF
68. Shen M, Xu Z, Xu W, Jiang K, Zhang F, Ding Q, et al. Inhibition of ATM reverses EMT and decreases metastatic potential of cisplatin-resistant lung cancer cells through JAK/STAT3/PD-L1 pathway. J Exp Clin Cancer Res 2019;38:149.
PUBMED | CROSSREF

69. Kang W, Tong JH, Chan AW, Zhao J, Dong Y, Wang S, et al. Yin Yang 1 contributes to gastric carcinogenesis and its nuclear expression correlates with shorter survival in patients with early stage gastric adenocarcinoma. J Transl Med 2014;12:80.
PUBMED | CROSSREF

70. Bonavida B. Therapeutic YY1 inhibitors in cancer: ALL in ONE. Crit Rev Oncog 2017;22:37-47.
PUBMED | CROSSREF

71. Keld R, Guo B, Downey P, Cummins R, Gulmann C, Ang YS, et al. PEA3/ETV4-related transcription factors coupled with active ERK signalling are associated with poor prognosis in gastric adenocarcinoma. Br J Cancer 2011;105:124-130.
PUBMED | CROSSREF

72. Manicum T, Ni F, Ye Y, Fan X, Chen BC. Prognostic values of *E2F* mRNA expression in human gastric cancer. Biosci Rep 2018;38:BSR20181264.
PUBMED | CROSSREF

73. Xie Y, Wang C, Li L, Ma Y, Yin Y, Xiao Q. Overexpression of E2F-1 inhibits progression of gastric cancer in vitro. Cell Biol Int 2009;33:640-649.
PUBMED | CROSSREF

74. Nishi M, Batsaikhan BE, Yoshikawa K, Higashijima J, Tokunaga T, Takasu C, et al. High STAT4 expression indicates better disease-free survival in patients with gastric cancer. Anticancer Res 2017;37:6723-6729.
PUBMED

75. Teng Y, Cang B, Mao F, Chen W, Cheng P, Peng L, et al. Expression of ETS1 in gastric epithelial cells positively regulate inflammatory response in *Helicobacter pylori*-associated gastritis. Cell Death Dis 2020;11:498.
PUBMED | CROSSREF

76. Spiotto MT, Banh A, Papandreou I, Cao H, Galvez MG, Gurtner GC, et al. Imaging the unfolded protein response in primary tumors reveals microenvironments with metabolic variations that predict tumor growth. Cancer Res 2010;70:78-88.
PUBMED | CROSSREF

77. Dai W, Li Q, Liu BY, Li YX, Li YY. Differential networking meta-analysis of gastric cancer across Asian and American racial groups. BMC Syst Biol 2018;12 Suppl 4:51.
PUBMED | CROSSREF

78. Rong H, Gu S, Zhang G, Kang L, Yang M, Zhang J, et al. MiR-2964a-5p binding site SNP regulates *ATM* expression contributing to age-related cataract risk. Oncotarget 2017;8:84945-84957.
PUBMED | CROSSREF

79. Sandhu V, Bowitz Lothe IM, Labori KJ, Skrede ML, Hamfjord J, Dalsgaard AM, et al. Differential expression of miRNAs in pancreatobiliary type of periampullary adenocarcinoma and its associated stroma. Mol Oncol 2016;10:303-316.
PUBMED | CROSSREF

80. Moi L, Braaten T, Al-Shibli K, Lund E, Busund LR. Differential expression of the miR-17-92 cluster and miR-17 family in breast cancer according to tumor type; results from the Norwegian Women and Cancer (NOWAC) study. J Transl Med 2019;17:334.
PUBMED | CROSSREF

81. Wilkening S, Chen B, Bermejo JL, Canzian F. Is there still a need for candidate gene approaches in the era of genome-wide association studies? Genomics 2009;93:415-419.
PUBMED | CROSSREF

82. Jorgensen TJ, Ruczinski I, Kessing B, Smith MW, Shugart YY, Alberg AJ. Hypothesis-driven candidate gene association studies: practical design and analytical considerations. Am J Epidemiol 2009;170:986-993.
PUBMED | CROSSREF

83. Gorlov IP, Gorlova OY, Sunyaev SR, Spitz MR, Amos CI. Shifting paradigm of association studies: value of rare single-nucleotide polymorphisms. Am J Hum Genet 2008;82:100-112.
PUBMED | CROSSREF